



Published in final edited form as:

*Ann Biomed Eng.* 2015 November ; 43(11): 2642–2651. doi:10.1007/s10439-015-1315-6.

## Reducing Neointima Formation in a Swine Model with IVUS and Sirolimus Microbubbles

Joseph P. Kilroy<sup>1</sup>, Ali H. Dhanaliwala<sup>1</sup>, Alexander L. Klibanov<sup>1,2</sup>, Douglas K. Bowles<sup>3</sup>, Brian R. Wamhoff<sup>4</sup>, and John A. Hossack<sup>1</sup>

<sup>1</sup>Department of Biomedical Engineering, University of Virginia, Charlottesville, VA 22908, USA

<sup>2</sup>School of Medicine, University of Virginia, Charlottesville, VA 22908, USA

<sup>3</sup>Department of Veterinary Sciences, University of Missouri, Columbia, MO, USA

<sup>4</sup>HemoShear, LLC, Charlottesville, VA 22903, USA

### Abstract

Potent therapeutic compounds with dose dependent side effects require more efficient and selective drug delivery to reduce systemic drug doses. Here, we demonstrate a new platform that combines intravascular ultrasound (IVUS) and drug-loaded microbubbles to enhance and localize drug delivery, while enabling versatility of drug type and dosing. Localization and degree of delivery with IVUS and microbubbles was assessed using fluorophore-loaded microbubbles and different IVUS parameters in *ex vivo* swine arteries. Using a swine model of neointimal hyperplasia, reduction of neointima formation following balloon injury was evaluated when using the combination of IVUS and sirolimus-loaded microbubbles. IVUS and microbubble enhanced fluorophore delivery was greatest when applying low amplitude pulses in the *ex vivo* model. In the *in vivo* model, neointima formation was reduced by 50% after treatment with IVUS and the sirolimus-loaded microbubbles. This reduction was achieved with a sirolimus whole blood concentration comparable to a commercial drug-eluting stent (0.999 ng/mL). We anticipate this therapy will find clinical use localizing drug delivery for numerous other diseases in addition to serving as an adjunct to stents in treating atherosclerosis.

### Keywords

Atherosclerosis; Ultrasound; Neointimal hyperplasia; Angioplasty

## INTRODUCTION

Coronary artery disease (CAD) is a leading cause of death worldwide.<sup>19,58</sup> Percutaneous coronary intervention (PCI), the mechanical restoration of blood flow in occluded arteries,

---

Address correspondence to John A. Hossack, Department of Biomedical Engineering, University of Virginia, Charlottesville, VA 22908, USA. jh7fj@virginia.edu, jpk4y@virginia.edu.

ELECTRONIC SUPPLEMENTARY MATERIAL

The online version of this article (doi:10.1007/s10439-015-1315-6) contains supplementary material, which is available to authorized users.

provides a minimally invasive technique to treat CAD. However, PCI can result in neointimal hyperplasia, an over proliferation of smooth muscle cells at the site of angioplasty, which induces restenosis and the need for target lesion revascularization (TLR). The drug-eluting stent (DES) has improved TLR, reduced mortality, and improved patient outcomes by providing localized antiproliferative therapy following angioplasty.<sup>18</sup> Localizing drug delivery has enabled clinical adoption of potent therapeutic compounds that were previously limited in use due to undesired and significant side effects when delivered systemically.<sup>36</sup> For example, the macrolide sirolimus provides no efficacy when administered orally to prevent neointimal hyperplasia and poses the risk of side effects including immunosuppression.<sup>7</sup> However, when localized by loading on a DES, sirolimus reduces in-stent restenosis with few side effects.<sup>18</sup> Despite these benefits, 70% of all DES are deployed in off-label lesions, which result in increased risk of death, myocardial infarction, and TLR as compared to bare metal stents (BMS).<sup>8,37,39,52</sup> Furthermore, state of the art DES technology provides only limited drug and dosing options that offer incomplete drug coverage of the target lesion.

In this work, we present preliminary data suggesting the combination of IVUS and microbubbles can reduce neointimal hyperplasia following PCI. We believe the combination of ultrasound and drug-loaded microbubbles can improve overall flexibility by tailoring drug selection, dose selection, and spatial delivery of antiproliferative therapy following PCI. The combination of ultrasound and microbubbles simultaneously localizes and enhances therapeutic uptake.<sup>31,32,42</sup>

Microbubbles, an ultrasound contrast agent and drug delivery vehicle, are comprised of a gas core surrounded by a lipid shell that can be loaded with molecules for delivery (e.g., fluorophores, drugs, genes, stem cells<sup>55</sup>). Importantly, microbubble oscillations enhance drug delivery by causing the transient permeabilization of the cell membrane.<sup>15</sup> This localizes enhancement of drug delivery within the ultrasound beam. In one study, this enhanced drug delivery decreased the sirolimus dose required to reduce neointima formation following PCI by tenfold.<sup>42,45</sup> In light of these benefits, we have developed an IVUS and microbubble drug delivery strategy, illustrated in Fig. 1. Here, we demonstrate this new technique for drug delivery within the vasculature, focusing on its application for the prevention of neointimal hyperplasia following balloon injury in a swine model.

## MATERIALS AND METHODS

### Microbubbles: Sirolimus and DiI Delivery Vehicles

Microbubbles (MBs) were formulated as described previously.<sup>42</sup> Briefly, an aqueous micellar dispersion of phosphatidylcholine (2 mg/mL) (Avanti Lipids, Alabaster, AL, USA), polyethylene glycol stearate (2 mg/mL) (Sigma Chemical Co., St. Louis, MO, USA), and either sirolimus (0.4 mg/mL, Chemwerth Inc, Woodbridge, CT, USA) or 1,1'-dioctadecyl-3,3,3'-tetramethylindocarbocyanine (DiI, Molecular Probes, Eugene, OR, USA,  $\approx$ 1% molar ratio DiI:DSPC, MW: 925.49 Da; Ex\Em: 549\565) was prepared in saline. This dispersion was sonicated in the presence of decafluorobutane (DFB, Flura, Newport, TN, USA). Prior to use, microbubbles were washed *via* centrifugation to remove excess lipids and DiI/sirolimus. A 200  $\mu$ g dose, similar to the dose of a commercial DES,

was selected to determine the total number of sirolimus-loaded microbubbles to infuse.<sup>1,9</sup> The sirolimus concentration of the prepared microbubbles was previously determined through HPLC-mass spectrometry analysis to be 29 ng/10<sup>6</sup> MBs.<sup>45</sup> The microbubbles had an average diameter of 2.2  $\mu$ m.

### Intravascular Ultrasound

In order to displace the microbubbles from the catheter to the vessel wall (Fig. 1),<sup>30</sup> a custom 5.3 MHz mechanically rotated single element intravascular ultrasound (IVUS) transducer was designed and fabricated. A center frequency of 5 MHz, lower than a commercial imaging IVUS catheter, was selected to provide better acoustic radiation force displacement and sonoporation effects with microbubbles.<sup>11,28,29</sup> The insonation pulse applied to the transducer consisted of a displacement pulse and/or a burst pulse (1 or 2 MPa) based on previously investigated ultrasound conditions.<sup>13,44,47</sup> The displacement pulse was a long (500 cycle), high duty cycle (50%), low peak negative pressure (PNP = 600 kPa) pulse to displace microbubbles from flow to the vessel wall. The burst pulse was a short (50 cycle), low duty cycle (1%), high peak negative pressure (PNP = 1 or 2 MPa) pulse designed to disrupt microbubbles and induce drug release and uptake by cells. The increase in temperature at the face of the IVUS transducer temperature was measured while driving the transducer with the 50% duty cycle, PNP = 600 kPa pulse for 20 min while in a beaker of water. Over three trials a maximum increase of 1.8 °C was measured.

### Fluorophore Delivery in Ex Vivo Swine Arteries

An experimentally verified *ex vivo* model of fluorophore delivery in swine arteries was used to optimize the ultrasound parameters for IVUS and microbubble enhanced delivery.<sup>22</sup> DiI microbubbles dispersed in bovine blood (40–45% hematocrit) at a concentration of 2.25  $\times$  10<sup>6</sup> MB/mL were infused into common carotid arteries harvested from swine at a local abattoir.<sup>40</sup> Human coronary artery flow was modeled by infusing blood (105 mL/min flow rate) into the arteries (average diameter 5.78  $\pm$  0.1 mm). The flow rate was selected to correspond to a laminar flow velocity similar to that of the average peak velocity of the human coronary artery of 13.3 cm/s.<sup>25</sup>

Four treatments were applied to four different longitudinal locations within each artery (Table 1, Supplemental Fig. 1B). Each longitudinal location received four consecutive 15 s insonations divided between displacement and burst pulses. Each of the four treatments (Table 1) was repeated in three arteries for a total of 12 treated artery sections.

Following treatment, the arteries were cut longitudinally and imaged *en face*. Arteries were imaged on a confocal microscope (LSM700, Carl Zeiss Microscopy LLC, Thornwood, NY, USA) with a 555 nm excitation. A mosaic of images along the circumference of each treatment region was collected using the ZEN software (Zeiss Microscopy LLC, Thornwood, NY, USA).

### Neointima Reduction Following Balloon Injury in Swine

Eight domestic Yorkshire farm pigs were used as a model of balloon injury in the coronary artery due to the anatomical similarity of swine to human coronary arteries.<sup>49</sup> Balloon injury

was performed in 2–3 coronary arteries in each pig. Vessel diameter was measured by angiography and inflation pressure was selected such that the balloon (Maverick 12–20 mm length, Boston Scientific, Natick, MA, USA) was 1.3× the artery diameter. The 1.3× inflation diameter was selected to maximize vessel injury and induce neointima formation.<sup>17</sup> The balloon was inflated three times for 30 s with a 1 min rest between inflations.<sup>54</sup> Animal protocols were approved by the University of Missouri Animal Care and Use Committee in accordance with the “Principles for the Utilization and Care of Vertebrate Animals Used in Testing, Research and Training.”

### **Sirolimus-Loaded Microbubble Treatment**

After injury, the IVUS transducer was positioned within the injured segment of the vessel under angiographic guidance. Arteries were treated with (MB + IVUS) or without IVUS application (MB – IVUS). In arteries treated with IVUS, the optimal acoustic parameters, as determined from the *ex vivo* experiments, were applied (5 MHz center frequency, 500 cycles, 50% duty cycle, PNP = 600 kPa) as the IVUS transducer was translated longitudinally 2 mm/min and rotated at a rate of 250 RPM within the catheter sheath.

During IVUS treatment, a dispersion of sirolimus-loaded microbubbles (5 mL at  $1.38 \times 10^9$  MB/mL) was infused into the catheter lumen at a rate of 1 mL/min while agitating the syringe to prevent buoyancy-based separation of the microbubbles. The microbubbles then exited through an ejection port at the distal end of the catheter proximal to the transducer into the blood stream. IVUS treatment was randomized among vessels and applied to an average vessel length of  $14.7 \pm 2.6$  mm. Venous whole blood samples were drawn from three pigs to measure the serum concentration of sirolimus. Samples were drawn before treatment, after each vessel was treated, and 24 h after the procedure. The sirolimus concentration of these samples was measured using high performance liquid chromatography (HPLC).

### **Histology**

Twenty-eight days after injury, the pigs were euthanized and their hearts were removed and placed in Krebs bicarbonate solution during coronary dissection. Injured segments were excised after identification based on anatomical landmarks from angiograms. After dissection, arteries were fixed in a 10% paraformaldehyde solution. Verhoff Van Gieson (VVG)-stain was applied and images of sections were obtained.

Analysis of vessel morphometry was performed using ImageJ software by a blinded observer.<sup>2</sup> Intimal and medial areas were measured, using the luminal and internal elastic lamina as the boundary of the intimal area. The rupture length (RL) and the internal elastic lamina length (IEL) were measured and used to determine the rupture index ( $RI = RL/IEL$ ).<sup>4</sup> The rupture length was defined as the length of discontinuity of the injured internal elastic lamina. The intima to media ratio was calculated as a measure of neointima formation ( $IM = \text{intimal area}/\text{medial area}$ ). Efficacy was measured by normalizing IM to RI to account for the degree of vessel disruption ( $IM/RI$ ).<sup>4,53</sup> Analysis was performed on 5 MB – IVUS arteries and 7 MB + IVUS arteries. Analysis was performed on both the average IM/RI of all

sections within each artery (Mean IM/RI in Fig. 2a) and on the section with the largest IM from each artery (Maximum IM in Fig. 2a).

### Statistical Analysis

Analysis of variance (ANOVA) was applied to compare the fluorescence intensity increase across *ex vivo* artery segments treated with different ultrasound parameters. A significance value ( $p$ ) < 0.01 was considered significant with a Bonferroni correction applied ( $p$ /number of comparisons). A Wilcoxon Rank-Sum test was applied to compare IM/RI following treatment with and without therapeutic ultrasound for *in vivo* sirolimus delivery experiments. A  $p$  < 0.05 was considered significant.

## RESULTS

### Fluorophore Delivery in Ex Vivo Swine Arteries

In *ex vivo* swine arteries treated with IVUS and DiI microbubbles, a sixfold increase in fluorescence intensity was measured when applying displacement pulses alone. Under the same flow and microbubble conditions, no increase was measured when applying bursting pulses ( $6.01 \pm 2.01$  vs.  $0.66 \pm 0.15$  fold, respectively,  $p < 0.01$ ; Fig. 2a). Microscopy of vessel segments verifies the localization of the DiI delivery, with fluorescence detected in a band along the region of the artery wall that received ultrasound treatment (Figs. 2b and 2c).

### Reduction of Neointima Formation: Morphometric Analysis

Following balloon injury and treatment with IVUS and sirolimus-loaded microbubbles, vessel intima to media ratio decreased by 50% on average (Table 2). When normalized by the degree of injury, a decrease in IM/RI of 33% was measured on average (Table 2; Fig. 3a— $3.90 \pm 0.43$  vs.  $5.82 \pm 1.28$ ,  $p = 0.030$ ) in arteries treated with IVUS and sirolimus-loaded microbubbles (Fig. 4b) as compared to arteries treated with sirolimus-loaded microbubbles alone (Fig. 4a). Comparing only the histological sections with the greatest IM from each vessel (maximum IM), mean IM/RI decreased by 50% (Table 2; Fig. 3a— $2.14 \pm 0.31$  vs.  $8.63 \pm 1.28$ ,  $p = 0.0055$ ).

### Reduction of Neointima Formation: Whole Blood Drug Concentration

The peak sirolimus serum concentration after treating three arteries with sirolimus-loaded microbubbles was  $0.999 \pm 0.129$  ng/mL (Fig. 3b). A trend of decreasing sirolimus concentration is apparent 24 h after the procedure with a half life of 60 h, which is within the reported range for humans.<sup>60</sup>

## DISCUSSION

The present study is the first preclinical application of IVUS and drug-loaded microbubbles for the prevention of neointimal hyperplasia in a large animal model. IVUS and microbubble enhanced sirolimus delivery was compared to treatment with sirolimus-loaded microbubbles alone, 28 days after angioplasty. Ultrasound application improved the intima to media ratio, suggesting enhanced drug delivery within the vessels due to IVUS and microbubbles (Fig. 5).

In the *ex vivo* artery study, an increase in fluorescence intensity was measured in arteries when a displacement pulse was applied to the microbubbles. This fluorescence intensity increase is likely due to enhanced DiI uptake in endothelial cells of the artery because no denuding process has been performed. We hypothesize two potential mechanisms for the enhanced delivery in the displacement cases. First, it has been previously demonstrated that microbubble displacement in blood requires a higher duty cycle ultrasound pulse than in water or saline.<sup>30,40</sup> The lower duty cycle for the bursting pulses alone may have been insufficient to displace the microbubbles to the vessel wall preventing DiI uptake into the tissue at the designated flow speeds and viscosities. Second, previous studies have documented the release of dye from within the microbubble shell without rupture due to lipid shedding<sup>5</sup> and the transient permeabilization of the membrane due to microstreaming.<sup>59</sup> Without microbubble bursting, the enhanced uptake of dye may have been caused by more sustained release due to lipid shedding with persistent microbubbles continuing to permeabilize the cell membrane.

A sirolimus dose comparable to the state of the art for antiproliferative therapy, a commercial DES (200 µg<sup>9</sup>), was used in this study. With this dose, a 33–50% reduction in neointima formation was measured. As a lone therapy, the ultrasound activated sirolimus-loaded microbubbles yielded reductions in neointimal formation in line with those of previous studies using drug-eluting stents or drug-eluting balloons, which ranged from 22 to 55%.<sup>23,33,38,51</sup> Other studies have used microbubbles without ultrasound to provide sirolimus delivery, but required a much higher dose of sirolimus to reduce neointimal hyperplasia.<sup>32</sup>

Sirolimus concentration within the blood following infusion of three arteries with sirolimus-loaded microbubbles was comparable to that found after implanting two drug-eluting stents (Cypher—1.05 ng/mL at 3.4 h).<sup>9</sup> When comparing whole blood concentration per artery, IVUS and drug-loaded microbubbles yield a lower concentration (0.38 ng/mL per infusion) when compared to two DES (0.5 ng/mL per stent). This decrease in sirolimus concentration of the blood may imply a greater drug uptake within the tissue due to sonoporation. Also important to note, is that the DES releases sirolimus over time while the microbubble delivery method delivers the sirolimus at one time. Previous studies have demonstrated improved reendothelialization with BMS as compared to DES,<sup>12,26,27</sup> suggesting that a reduction in overall sirolimus dose or period of sirolimus exposure may also improve reendothelialization following balloon injury.

The results of this study must be understood in terms of its scale as a pilot. The experimental conditions tested in this study were selected based on results found in the literature.

Sirolimus alone has been studied through oral dosing and found to provide no therapeutic benefit in patients.<sup>7</sup> Another study used co-injection of microbubbles and sirolimus without ultrasound to reduce intimal area by 62% with with a total dose of 2 mg per vessel, tenfold higher than the dose administered in this study.<sup>32</sup> When ultrasound alone is applied above the FDA regulated MI neointima formation can be reduced,<sup>17</sup> however ultrasound alone below the FDA regulated MI does not provide any reduction in neointima formation.<sup>42</sup> Measurement of the whole blood concentration of sirolimus provided an indication of procedure safety and trended towards a decrease, but the study was limited in terms of

sample size and no statistically significant difference in whole blood concentration of sirolimus was measured in comparison to the Cypher DES.

This study has focused on the use of drug-loaded microbubbles and ultrasound for enhanced drug delivery. However, other studies have demonstrated that co-injection (simultaneous injection of plain microbubbles and drug) with and without ultrasound can also enhance drug and fluorophore delivery.<sup>13,32</sup> In this study, sirolimus was loaded into the microbubble shell because it ensures that the drug and the microbubble are together for delivery. By loading drug into the microbubble shell, we ensure that acoustic radiation force guides both the microbubble and the drug to the vessel wall for delivery. Microbubble proximity is critical to sonoporation,<sup>16,24,56</sup> and by guiding both the microbubble and drug to the site of delivery, better control of delivery can be achieved while concentrating drug at the cell. However, a direct *in vivo* comparison must be made between direct intravenous infusion of drug, ultrasound enhanced intravenous infusion, and microbubble and ultrasound enhanced drug delivery (co-injection and drug-loading of microbubbles) to verify these benefits of drug-loading.

Previous studies demonstrated enhanced drug uptake in animal models using transcutaneous ultrasound and microbubbles. However, these studies infused microbubbles and drug systemically while applying high PNP ultrasound (> 1 MPa).<sup>31,42,50</sup> As a result of the catheter based approach and the proximity to the lesion, we can infuse the drug-loaded microbubbles at the location of treatment, reducing overall drug dose while using a lower ultrasound pressure (600 kPa).

Although IVUS and microbubble enhanced antiproliferative delivery decreased neointimal formation by 50%, this effect may be enhanced by the mechanical support of stenting.<sup>18</sup> By augmenting DES and bare metal stents (BMS) with an adjunct therapy such as IVUS with sirolimus-loaded microbubbles, patient outcomes following PCI may be improved. Designing drug delivery to address specific DES off-label lesions may reduce the risk of death, MI, and TVR by reducing systemic antiproliferative drug dose and enhancing drug uptake, thereby improving reendothelialization.<sup>6,21,46</sup> The combination of ultrasound and MBs has been demonstrated to enhance drug uptake by transiently permeabilizing the cell membrane.<sup>3,16,28</sup> Enhanced drug delivery may enable shorter drug delivery duration and lower required doses for therapeutic effect.<sup>43</sup>

Two benefits of enhanced short drug delivery instead of sustained duration therapy from DES are reduced dual antiplatelet therapy (DAPT) duration and quicker healing (i.e., reendothelialization). Reducing antiproliferative therapy duration with IVUS and MBs may enable shorter DAPT duration, reducing cost and risk of bleeding complications<sup>14,34,41</sup> while still preventing restenosis. Delivering drug in a single localized dose with IVUS and MBs instead of prolonged therapy with a DES can improve injury healing while preventing restenosis, resulting in a quicker recovery and reducing complications associated with slow healing such as thrombosis.<sup>26,27,35</sup> The stent would provide mechanical support of the vessel following therapy, a component included in previous preclinical studies, while the sirolimus-loaded microbubble delivery may provide more uniform delivery between stent struts and enable delivery tailored to the specific patient.

IVUS already has a role diagnosing and guiding vascular interventions.<sup>48</sup> Twenty percent of PCI procedures use IVUS to guide intervention<sup>10</sup> and IVUS has been proven to improve patient outcomes following PCI.<sup>57</sup> These strengths make IVUS ideally positioned to deliver therapy to prevent post-PCI restenosis. However, current clinical catheters are not optimized for ultrasound and microbubble enhanced drug delivery due to their high frequency and low power output.<sup>20</sup> In order to overcome this limitation, we designed and fabricated a custom IVUS catheter with a lower center frequency, capable of insonating microbubbles to enhance drug delivery.

In addition to comparable efficacy and safety, IVUS and sirolimus-loaded microbubble delivery can provide versatility that existing drug delivery techniques do not. Current stent technology is limited to select drugs, doses, and strut-defined delivery patterns. These limited stent options result in limited treatment options. By complementing stents with IVUS and microbubble enhanced delivery drug choice, dosing, and coverage can be adapted to the patient's needs and the current clinical best practices. IVUS and microbubble enhanced drug delivery also raises the possibility of new treatments, including multi-drug therapies, molecularly targeted therapies, and gene therapy. Looking beyond PCI, other interventions and therapies may also benefit from the localized enhancement of drug delivery.

## CONCLUSIONS

This preclinical study using a DES comparable sirolimus dose demonstrates that IVUS and microbubble enhanced drug delivery can improve antiproliferative drug delivery within the vasculature. IVUS and sirolimus-loaded microbubbles may enable patient tailored drug delivery to improve post-PCI outcomes.

## Supplementary Material

Refer to Web version on PubMed Central for supplementary material.

## ACKNOWLEDGMENTS

The authors would like to acknowledge Gore Processing Inc. of Edinburg, VA for providing tissue samples and Jan Ivey and Darla Tharp, PhD for their assistance and technical expertise during the *in vivo* swine experiments. This work was supported by NIH National Heart Lung and Blood Institute award HL090700, National Institute of General Medical Sciences award T32GM008715, and the University of Virginia Coulter Translational Research Grant. The opinions expressed in this article are those of the authors and do not reflect any official position of the NIH.

## REFERENCES

1. Abbott Vascular. XIENCE Xpedition, XIENCE Xpedition SV, and XIENCE Xpedition LL Everolimus Eluting Coronary Stent Systems: Instructions for Use. 2012 [http://www.abbottvascular.com/static/cms\\_workspace/pdf/ifu/coronary\\_intervention/eIFU\\_Xience\\_Xpedition.pdf](http://www.abbottvascular.com/static/cms_workspace/pdf/ifu/coronary_intervention/eIFU_Xience_Xpedition.pdf).
2. Abramoff MD, Magelhaes PJ, Ram SJ. Image processing with ImageJ. *Biophotonics Int.* 2004; 11:36–42.
3. Bao S, Thrall BD, Miller DL. Transfection of a reporter plasmid into cultured cells by sonoporation in vitro. *Ultrasound Med. Biol.* 1997; 23:953–959. [PubMed: 9300999]



4. Bonan R, Paiement P, Scortichini D, Cloutier M-J, Leung TK. Coronary restenosis: evaluation of a restenosis injury index in a swine model. *Am. Heart J.* 1993; 126:1334–1340. [PubMed: 8249790]
5. Borden MA, Longo ML. Dissolution behavior of lipid monolayer-coated, air-filled microbubbles: effect of lipid hydrophobic chain length. *Langmuir.* 2002; 18:9225–9233.
6. Boston Scientific. ION Paclitaxel-Eluting Platinum Chromium Coronary Stent System: Directions For Use. 2012 [http://www.bostonscientific.com/templatedata/imports/collateral/eDFU/ion\\_dfu\\_90756361-01A\\_us.pdf](http://www.bostonscientific.com/templatedata/imports/collateral/eDFU/ion_dfu_90756361-01A_us.pdf).
7. Brara PS, Moussavian M, Grise MA, Reilly JP, Fernandez M, Schatz RA, Teirstein PS. Pilot trial of oral rapamycin for recalcitrant restenosis. *Circulation.* 2003; 107:1722–1724. [PubMed: 12665483]
8. Brodie BR, Stuckey T, Downey W, Humphrey A, Bradshaw B, Metzger C, Hermiller J, Krainin F, Juk S, Cheek B, Duffy P, Smith H, Edmunds J, Varanasi J, Simonton CA. Outcomes and complications with off-label use of drug-eluting stents results from the STENT (Strategic Transcatheter Evaluation of New Therapies) group. *JACC Cardiovasc. Interv.* 2008; 1:405–414. [PubMed: 19463338]
9. Cordis. Instructions for Use: CYPHER Sirolimus-eluting Coronary Stent on RAPTOR Over-the-Wire Delivery System. 2011 <http://www.cordislabeling.com/pdf/10056734.pdf>.
10. Dattilo PB, Prasad A, Honeycutt E, Wang TY, Messenger JC. Contemporary patterns of fractional flow reserve and intravascular ultrasound use among patients undergoing percutaneous coronary intervention in the United States: insights from the national cardiovascular data registry. *J. Am. Coll. Cardiol.* 2012; 60:2337–2339. [PubMed: 23194945]
11. Dayton PA, Allen JS, Ferrara KW. The magnitude of radiation force on ultrasound contrast agents. *J. Acoust. Soc. Am.* 2002; 112:2183–2192. [PubMed: 12430830]
12. de Prado AP, Pérez-Martínez C, Cuellas-Ramón C, Gonzalo-Orden JM, Regueiro-Purriños M, Martínez B, García-Iglesias MJ, Ajenjo JM, Altónaga JR, Diego-Nieto A, de Miguel A, Fernández-Vázquez F. Time course of reendothelialization of stents in a normal coronary swine model characterization and quantification. *Vet. Pathol. Online.* 2011; 48:1109–1117.
13. Dixon AJ, Dhanaliwala AH, Chen JL, Hossack JA. Enhanced intracellular delivery of a model drug using microbubbles produced by a microfluidic device. *Ultrasound Med. Biol.* 2013; 39:1267–1276. [PubMed: 23643062]
14. Eisenstein EL, Anstrom KJ, Kong DF, et al. Clopidogrel use and long-term clinical outcomes after drug-eluting stent implantation. *JAMA.* 2007; 297:159–168. [PubMed: 17148711]
15. Fan Z, Liu H, Mayer M, Deng CX. Spatiotemporally controlled single cell sonoporation. *Proc. Natl. Acad. Sci.* 2012; 109:16486–16491. [PubMed: 23012425]
16. Fan Z, Liu H, Mayer M, Deng CX. Spatiotemporally controlled single cell sonoporation. *Proc. Natl. Acad. Sci. USA.* 2012; 109:16486–16491. [PubMed: 23012425]
17. Fitzgerald PJ, Takagi A, Moore MP, Hayase M, Kolodgie FD, Corl D, Nassi M, Virmani R, Yock PG. Intravascular sonotherapy decreases neointimal hyperplasia after stent implantation in swine. *Circulation.* 2001; 103:1828–1831. [PubMed: 11294798]
18. Garg S, Serruys PW. Coronary stents: current status. *J. Am. Coll. Cardiol.* 2010; 56:S1–S42. [PubMed: 20797502]
19. Go AS, et al. Heart disease and stroke statistics—2014 update a report from the American Heart Association. *Circulation.* 2014; 129:e28–e292. [PubMed: 24352519]
20. Goertz DE, Frijlink ME, Tempel D, Bhagwandas V, Gisolf A, Krams R, de Jong N, van der Steen AFW. Subharmonic contrast intravascular ultrasound for vasa vasorum imaging. *Ultrasound Med. Biol.* 2007; 33:1859–1872. [PubMed: 17683850]
21. Guagliumi G, Musumeci G, Sirbu V, Bezerra HG, Suzuki N, Fiocca L, Matiashvili A, Lortkipanidze N, Trivisonno A, Valsecchi O, Biondi-Zoccai G, Costa MA. Optical coherence tomography assessment of in vivo vascular response after implantation of overlapping bare-metal and drug-eluting stents. *JACC Cardiovasc. Interv.* 2010; 3:531–539. [PubMed: 20488410]
22. Hallow D, Mahajan A, Prausnitz M. Ultrasonically targeted delivery into endothelial and smooth muscle cells in ex vivo arteries. *J. Control. Release.* 2007; 118:285–293. [PubMed: 17291619]
23. Heldman AW, Cheng L, Jenkins GM, Heller PF, Kim D-W, Ware M, Nater C, Hruban RH, Rezaei B, Abella BS, Bunge KE, Kinsella JL, Sollott SJ, Lakatta EG, Brinker JA, Hunter WL, Froehlich

- JP. Paclitaxel stent coating inhibits neointimal hyperplasia at 4 weeks in a porcine model of coronary restenosis. *Circulation*. 2001; 103:2289–2295. [PubMed: 11342479]
24. Hernot S, Klibanov AL. Microbubbles in ultrasound-triggered drug and gene delivery. *Adv. Drug Deliv. Rev.* 2008; 60:1153–1166. [PubMed: 18486268]
25. Hozumi T, Yoshida K, Akasaka T, Asami Y, Ogata Y, Takagi T, Kaji S, Kawamoto T, Ueda Y, Morioka S. Noninvasive assessment of coronary flow velocity and coronary flow velocity reserve in the left anterior descending coronary artery by Doppler echocardiography: comparison with invasive technique. *J. Am. Coll. Cardiol.* 1998; 32:1251–1259. [PubMed: 9809933]
26. Joner M, Finn AV, Farb A, Mont EK, Kolodgie FD, Ladich E, Kutys R, Skorija K, Gold HK, Virmani R. Pathology of drug-eluting stents in humans-delayed healing and late thrombotic risk. *J. Am. Coll. Cardiol.* 2006; 48:193–202. [PubMed: 16814667]
27. Joner M, Nakazawa G, Finn AV, Quee SC, Coleman L, Acampado E, Wilson PS, Skorija K, Cheng Q, Xu X, Gold HK, Kolodgie FD, Virmani R. Endothelial cell recovery between comparator polymer-based drug-eluting stents. *J. Am. Coll. Cardiol.* 2008; 52:333–342. [PubMed: 18652940]
28. Karshafian R, Bevan PD, Williams R, Samac S, Burns PN. Sonoporation by ultrasound-activated microbubble contrast agents: effect of acoustic exposure parameters on cell membrane permeability and cell viability. *Ultrasound Med. Biol.* 2009; 35:847–860. [PubMed: 19110370]
29. Kilroy JP, Klibanov AL, Wamhoff BR, Hossack JA. Intravascular ultrasound catheter to enhance microbubble-based drug delivery via acoustic radiation force. *IEEE Trans. Ultrason. Ferroelectr. Freq. Control.* 2012; 59:2156–2166. [PubMed: 23143566]
30. Kilroy JP, Patil AV, Rychak JJ, Hossack JA. An IVUS transducer for microbubble therapies. *IEEE Transactions Ultrason. Ferroelectr. Freq. Control.* 2014; 61:441–449.
31. Kinoshita M, McDannold N, Jolesz FA, Hynynen K. Noninvasive localized delivery of Herceptin to the mouse brain by MRI-guided focused ultrasound-induced blood–brain barrier disruption. *Proc. Natl. Acad. Sci.* 2006; 103:11719–11723. [PubMed: 16868082]
32. Kipshidze NN, Porter TR, Dargas G, Yazdi H, Tio F, Xie F, Hellings D, Wolfram R, Seabron R, Waksman R, Abizaid A, Roubin G, Iyer S, Colombo A, Leon MB, Moses JW, Iversen P. Novel site-specific systemic delivery of Rapamycin with perfluorobutane gas microbubble carrier reduced neointimal formation in a porcine coronary restenosis model. *Catheter. Cardiovasc. Interv.* 2005; 64:389–394. [PubMed: 15736246]
33. Klugherz BD, Llanos G, Lieuallen W, Kopia GA, Papandreou G, Narayan P, Sasseen B, Adelman SJ, Falotico R, Wilensky RL. Twenty-eight-day efficacy and pharmacokinetics of the sirolimus-eluting stent. *Coron. Artery Dis.* 2002; 13:183–188. [PubMed: 12131023]
34. Lagerqvist B, James SK, Stenestrand U, Lindbäck J, Nilsson T, Wallentin L. Long-term outcomes with drug-eluting stents versus bare-metal stents in Sweden. *N. Engl. J. Med.* 2007; 356:1009–1019. [PubMed: 17296822]
35. Liu H-T, Li F, Wang W-Y, Li X-J, Liu Y-M, Wang R-A, Guo W-Y, Wang H-C. Rapamycin inhibits re-endothelialization after percutaneous coronary intervention by impeding the proliferation and migration of endothelial cells and inducing apoptosis of endothelial progenitor cells. *Tex. Heart Inst. J.* 2010; 37:194. [PubMed: 20401293]
36. Moses MA, Brem H, Langer R. Advancing the field of drug delivery: taking aim at cancer. *Cancer Cell.* 2003; 4:337–341. [PubMed: 14667500]
37. Nakagawa Y, Kimura T, Morimoto T, Nomura M, Saku K, Haruta S, Muramatsu T, Nobuyoshi M, Kadota K, Fujita H, Tatami R, Shiode N, Nishikawa H, Shibata Y, Miyazaki S, Murata Y, Honda T, Kawasaki T, Doi O, Hiasa Y, Hayashi Y, Matsuzaki M, Mitsudo K. Incidence and risk factors of late target lesion revascularization after sirolimus-eluting stent implantation (3-year follow-up of the j-Cypher Registry). *Am. J. Cardiol.* 2010; 106:329–336. [PubMed: 20643241]
38. Nakazawa G, Finn AV, John MC, Kolodgie FD, Virmani R. The significance of preclinical evaluation of sirolimus-, paclitaxel-, and zotarolimus-eluting stents. *Am. J. Cardiol.* 2007; 100:S36–S44.
39. Niccoli G, Stefanini GG, Capodanno D, Crea F, Ambrose JA, Berg R. Are the culprit lesions severely stenotic? *JACC Cardiovasc. Imaging.* 2013; 6:1108–1114. [PubMed: 24135324]

40. Patil AV, Rychak JJ, Klivanov AL, Hossack JA. Real-time technique for improving molecular imaging and guiding drug delivery in large blood vessels: in vitro and ex vivo results. *Mol. Imaging*. 2011; 10:238–247. [PubMed: 21521555]
41. Pfisterer M, Brunner-La Rocca HP, Buser PT, Rickenbacher P, Hunziker P, Mueller C, Jeger R, Bader F, Osswald S, Kaiser C. Late clinical events after clopidogrel discontinuation may limit the benefit of drug-eluting stents: an observational study of drug-eluting versus bare-metal stents. *J. Am. Coll. Cardiol*. 2006; 48:2584–2591. [PubMed: 17174201]
42. Phillips LC, Dhanaliwala AH, Klivanov AL, Hossack JA, Wamhoff BR. Focused ultrasound-mediated drug delivery from microbubbles reduces drug dose necessary for therapeutic effect on neointima formation. *Arterioscler. Thromb. Vasc. Biol*. 2011; 31:2853–2855. [PubMed: 21960561]
43. Phillips LC, Dhanaliwala AH, Klivanov AL, Hossack JA, Wamhoff BR. Focused ultrasound-mediated drug delivery from microbubbles reduces drug dose necessary for therapeutic effect on neointima formation-brief report. *Arterioscler. Thromb. Vasc. Biol*. 2011; 31:2853–2855. [PubMed: 21960561]
44. Phillips LC, Klivanov AL, Wamhoff BR, Hossack JA. Targeted gene transfection from microbubbles into vascular smooth muscle cells using focused, ultrasound-mediated delivery. *Ultrasound Med. Biol*. 2010; 36:1470–1480. [PubMed: 20800174]
45. Phillips LC, Klivanov AL, Wamhoff BR, Hossack JA. Localized ultrasound enhances delivery of rapamycin from microbubbles to prevent smooth muscle proliferation. *J. Control. Release*. 2011; 154:42–49. [PubMed: 21549778]
46. Räber L, Jüni P, Löffel L, Wandel S, Cook S, Wenaweser P, Togni M, Vogel R, Seiler C, Eberli F, Lüscher T, Meier B, Windecker S. Impact of stent overlap on angiographic and long-term clinical outcome in patients undergoing drug-eluting stent implantation. *J. Am. Coll. Cardiol*. 2010; 55:1178–1188. [PubMed: 20298923]
47. Rahim A, Taylor SL, Bush NL, ter Haar GR, Bamber JC, Porter CD. Physical parameters affecting ultrasound/microbubble-mediated gene delivery efficiency in vitro. *Ultrasound Med. Biol*. 2006; 32:1269–1279. [PubMed: 16875960]
48. Sanz J, Fayad ZA. Imaging of atherosclerotic cardiovascular disease. *Nature*. 2008; 451:953–957. [PubMed: 18288186]
49. Schwartz RS, Edelman E, Virmani R, Carter A, Granada JF, Kaluza GL, Chronos NAF, Robinson KA, Waksman R, Weinberger J, Wilson GJ, Wilensky RL. Drug-eluting stents in preclinical studies updated consensus recommendations for preclinical evaluation. *Circ. Cardiovasc. Interv*. 2008; 1:143–153. [PubMed: 20031669]
50. Shortencarier MJ, Dayton PA, Bloch SH, Schumann PA, Matsunaga TO, Ferrara KW. A method for radiation-force localized drug delivery using gas-filled lipospheres. *IEEE Trans. Ultrason. Ferroelectr. Freq. Control*. 2004; 51:822–831. [PubMed: 15301001]
51. Speck U, Scheller B, Abramjuk C, Breitwieser C, Dobberstein J, Boehm M, Hamm B. Neointima inhibition: comparison of effectiveness of non-stent-based local drug delivery and a drug-eluting purpose: methods: results: conclusion. *Radiology*. 2006; 240:411–418. [PubMed: 16864669]
52. Stefanini GG, Serruys PW, Silber S, Khattab AA, van Geuns RJ, Richardt G, Buszman PE, Kelbæk H, van Boven AJ, Hofma SH, Linke A, Klauss V, Wijns W, Macaya C, Garot P, Di Mario C, Manoharan G, Kornowski R, Ischinger T, Bartorelli AL, Gobbens P, Windecker S. The impact of patient and lesion complexity on clinical and angiographic outcomes after revascularization with zotarolimus- and everolimus-eluting stents: a substudy of the RESOLUTE All Comers Trial (a randomized comparison of a zotarolimus-eluting stent with an everolimus-eluting stent for percutaneous coronary intervention). *J. Am. Coll. Cardiol*. 2011; 57:2221–2232. [PubMed: 21616282]
53. Tharp DL, Masseur I, Ivey J, Ganjam VK, Bowles DK. Endogenous testosterone attenuates neointima formation after moderate coronary balloon injury in male swine. *Cardiovasc. Res*. 2009; 82:152–160. [PubMed: 19181935]
54. Tharp DL, Wamhoff BR, Wulff H, Raman G, Cheong A, Bowles DK. Local delivery of the KCa3.1 blocker, TRAM-34, prevents acute angioplasty-induced coronary smooth muscle phenotypic modulation and limits stenosis. *Arterioscler. Thromb. Vasc. Biol*. 2008; 28:1084–1089. [PubMed: 18309114]

55. Toma C, Fisher A, Wang J, Chen X, Grata M, Leeman J, Winston B, Kaya M, Fu H, Lavery L, Fischer D, Wagner WR, Villanueva FS. Vascular endoluminal delivery of mesenchymal stem cells using acoustic radiation force. *Tissue Eng. Part A*. 2011; 17:1457–1464. [PubMed: 21247343]
56. Van Wamel A, Kooiman K, Harteveld M, Emmer M, ten Cate FJ, Versluis M, de Jong N. Vibrating microbubbles poking individual cells: drug transfer into cells via sonoporation. *J. Control. Release*. 2006; 112:149–155. [PubMed: 16556469]
57. Witzenbichler B, Maehara A, Weisz G, Neumann F-J, Rinaldi MJ, Metzger DC, Henry TD, Cox DA, Duffy PL, Brodie BR, Stuckey TD, Mazzaferri EL, Xu K, Parise H, Mehran R, Mintz GS, Stone GW. Relationship between intravascular ultrasound guidance and clinical outcomes after drug-eluting stents the assessment of dual antiplatelet therapy with drug-eluting stents (ADAPT-DES) study. *Circulation*. 2014; 129:463–470. [PubMed: 24281330]
58. World Health Organization. *World Health Statistics 2014*. 2014.
59. Wu J, Ross JP, Chiu J-F. Repairable sonoporation generated by microstreaming. *J. Acoust. Soc. Am*. 2002; 111:1460–1464. [PubMed: 11931323]
60. Zimmerman JJ, Kahan BD. Pharmacokinetics of sirolimus in stable renal transplant patients after multiple oral dose administration. *J. Clin. Pharmacol*. 1997; 37:405–415. [PubMed: 9156373]

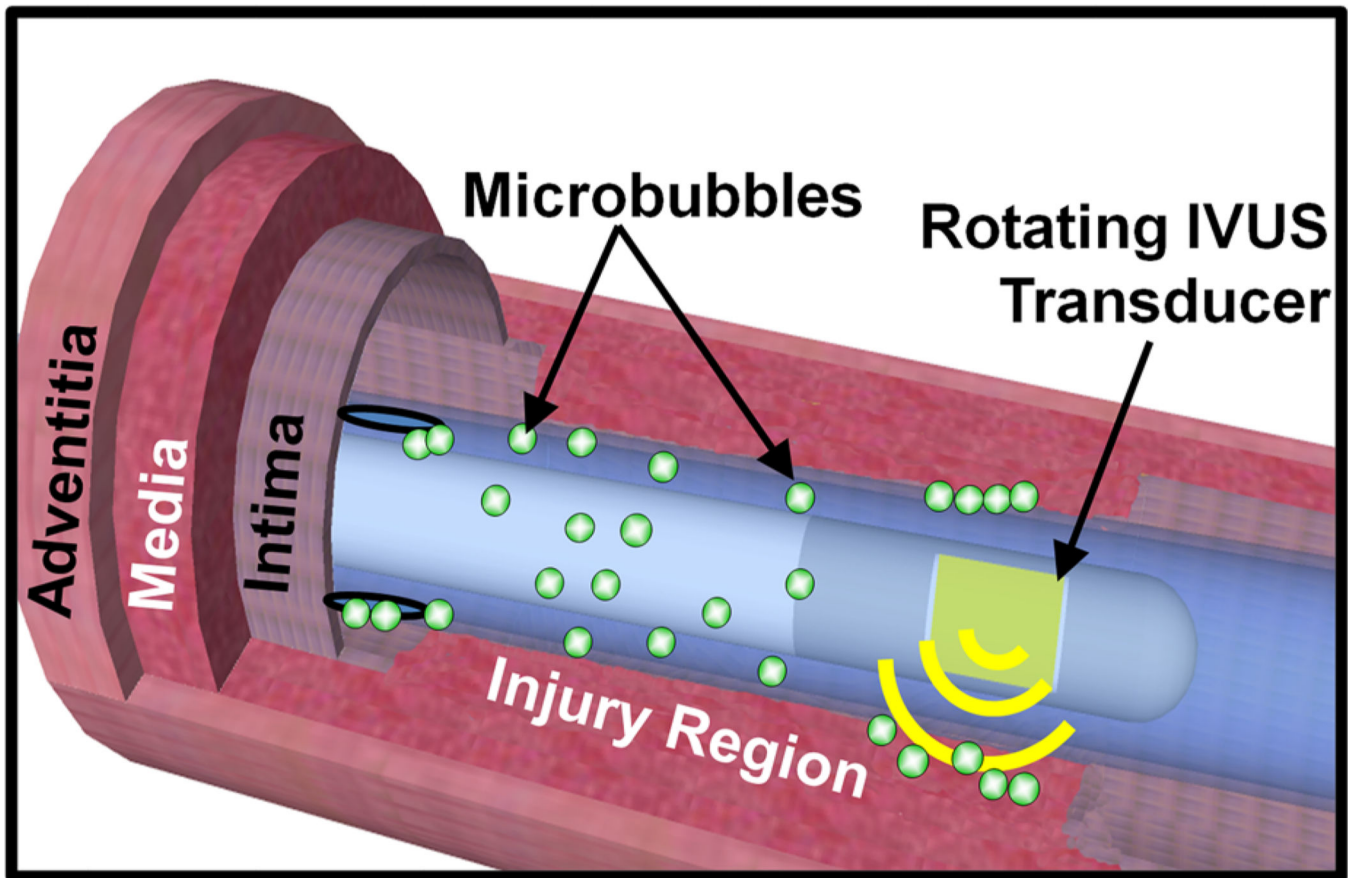


**FIGURE 1.** Schematic of ultrasound and microbubble enhanced delivery within the coronary artery. Sirolimus-loaded microbubbles are infused through the catheter while the IVUS transducer rotates and displaces the microbubbles to the vessel wall with ultrasound.

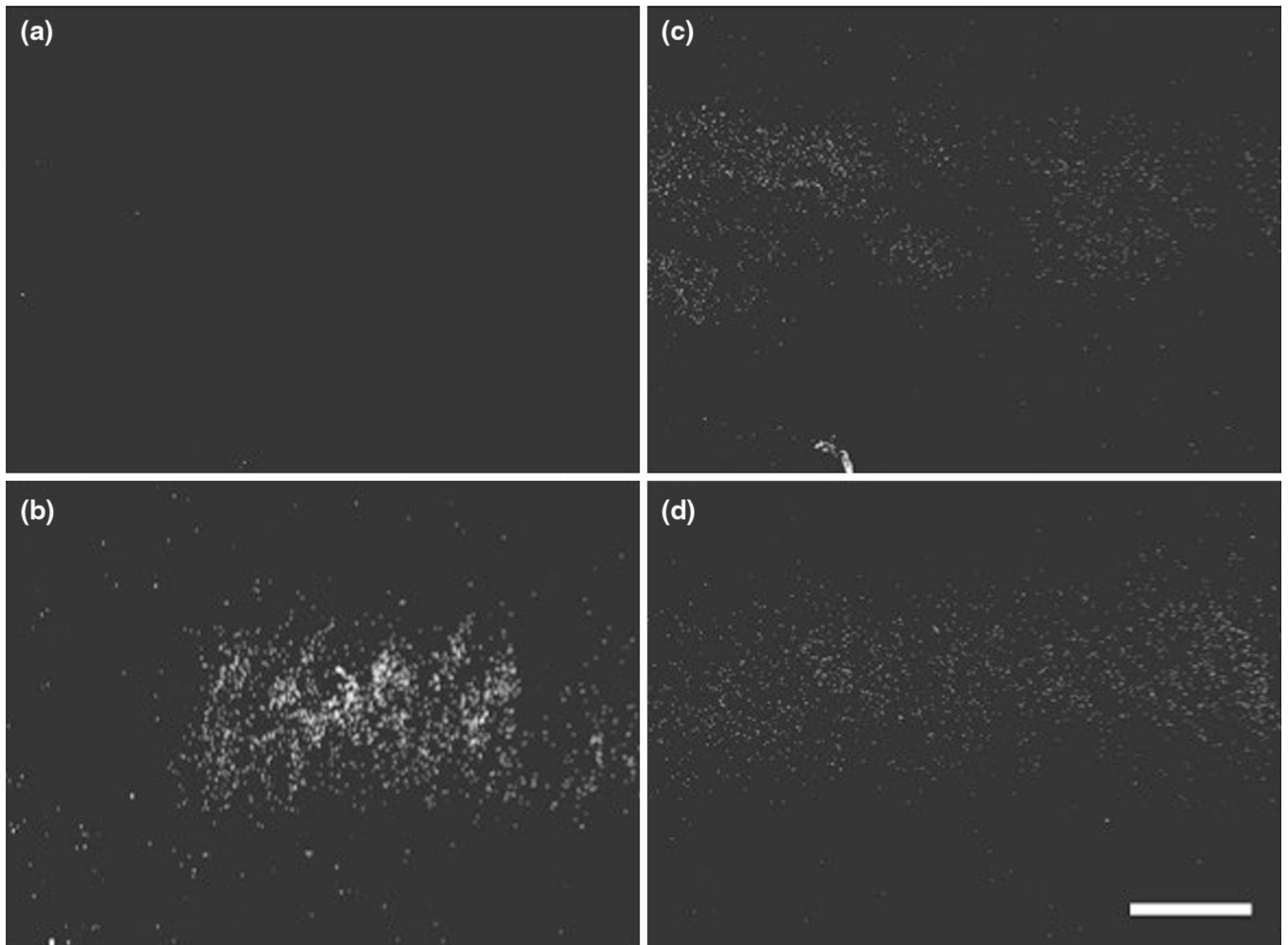


**FIGURE 2.** Microscope images following *ex vivo* fluorophore delivery with application of (a) 2 MPa burst pulse, (b) displacement pulse, (c) displacement and 1 MPa burst pulses, and (d) displacement and 2 MPa burst pulses. Artery circumference was from right to left in each image. Scale bar = 500  $\mu\text{m}$ .

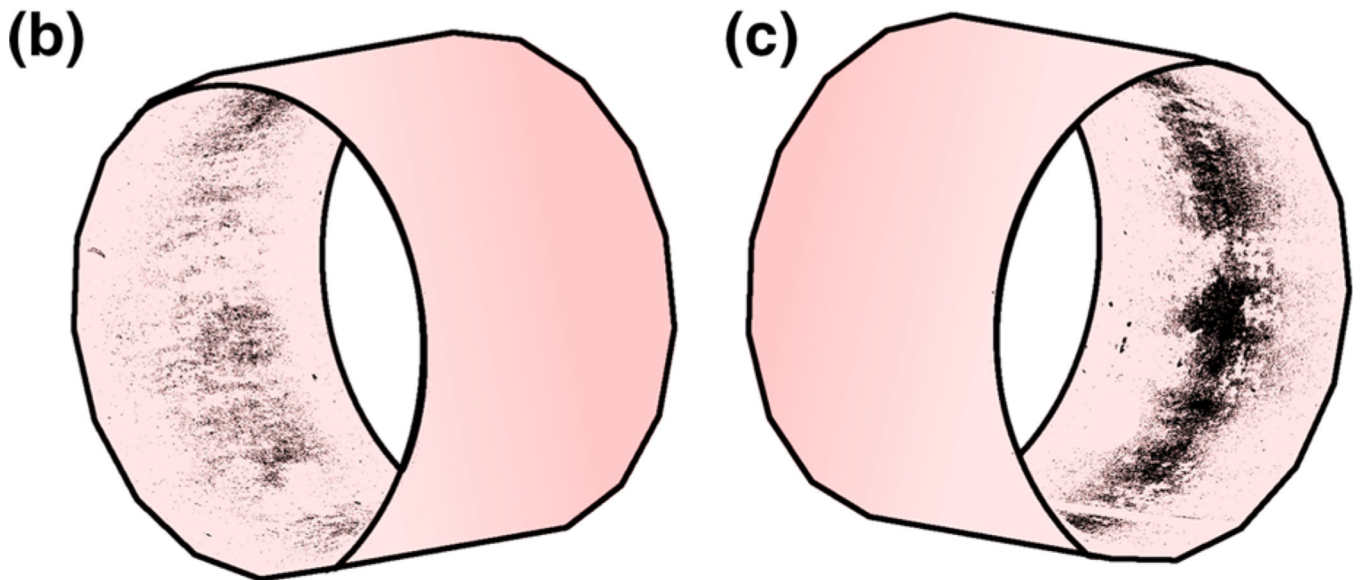
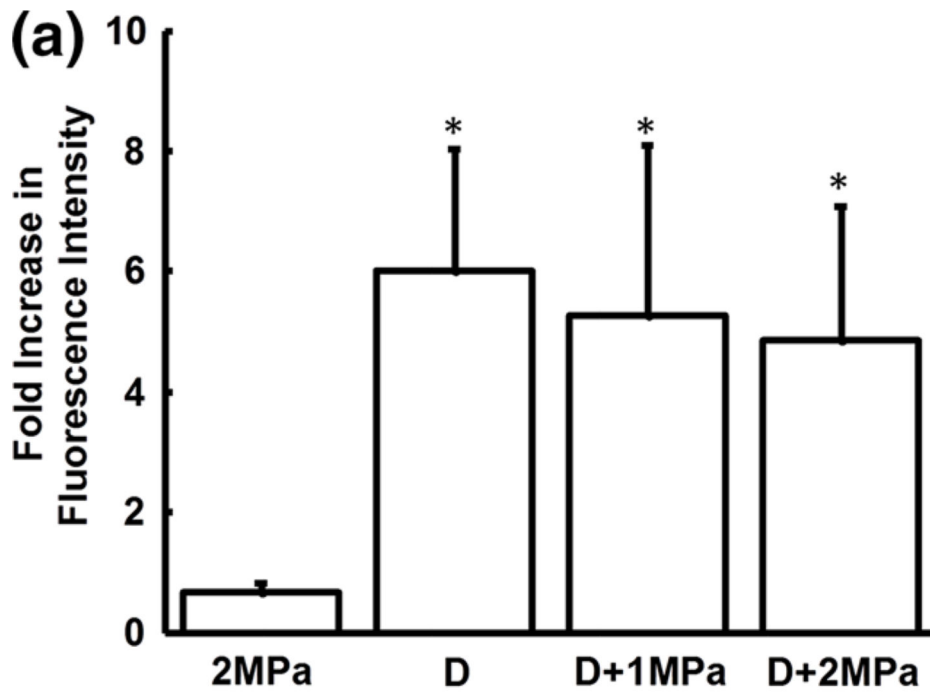


**FIGURE 3.**

(a) Comparison of the fluorescence intensity increase + standard deviation due to fluorophore delivery from microbubbles insonated by displacement ( $D$ ) and/or burst pulses (1 & 2 MPa;  $n = 3$ ). \* $p < 0.01$  for compared to 2 MPa. (b–c) Two perspectives of the *ex vivo* artery fluorescence after delivery, mapped on a cylinder.

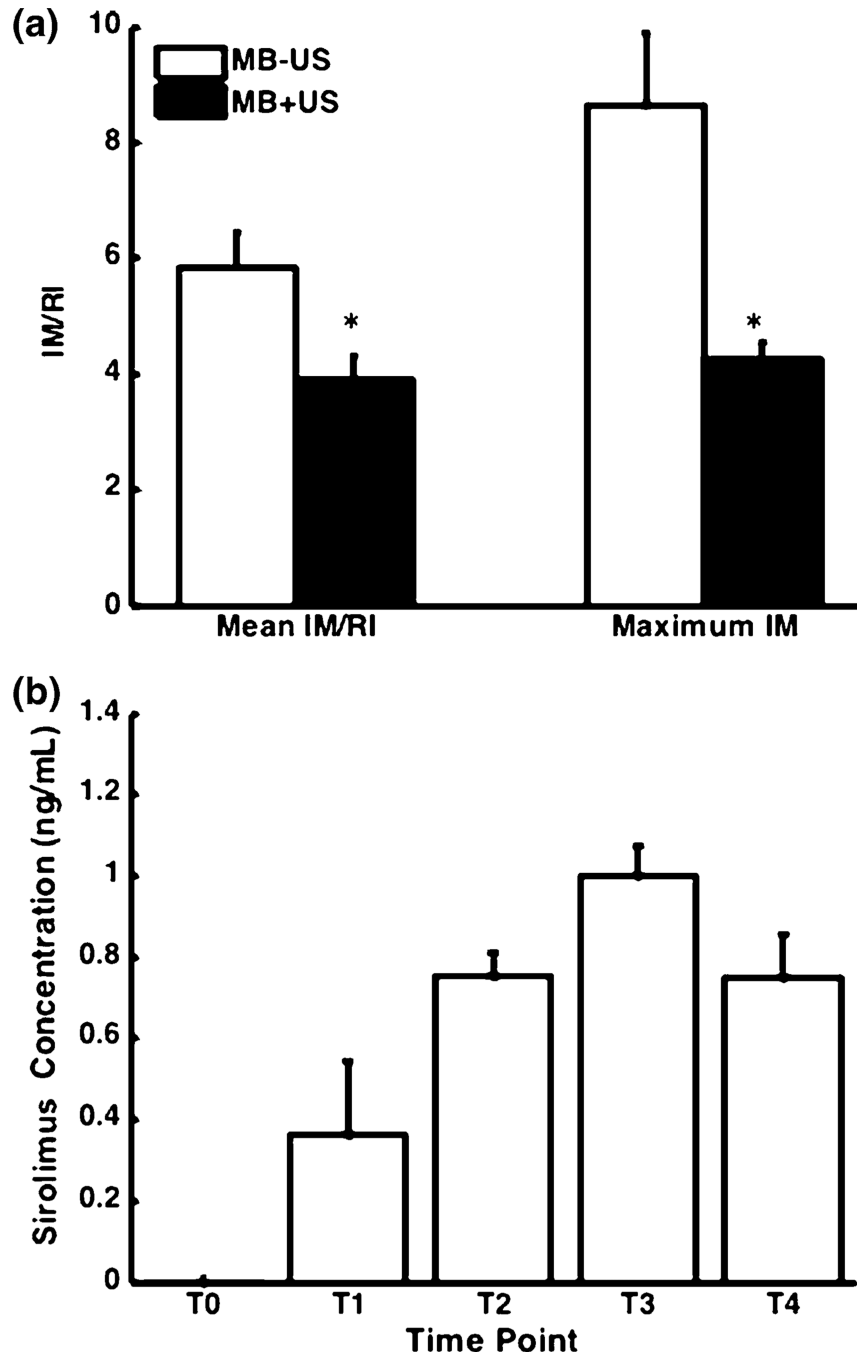


**FIGURE 4.**

(a) Intima to media (IM) normalized to rupture index (RI) + standard error of the mean with ( $n = 5$ ) and without ultrasound ( $n = 7$ ). *Left*—Mean IM/RI across all sections. *Right*—mean IM/RI of the histology sections with the greatest IM ratio from each vessel.  $*p < 0.05$  compared with no ultrasound application when testing with the Wilcoxon Rank-Sum test. (b) Serum concentration of sirolimus measured before treatment (T0), after treating each vessel (T1–3), and 24 h after treatment (T4).  $N = 3$ .



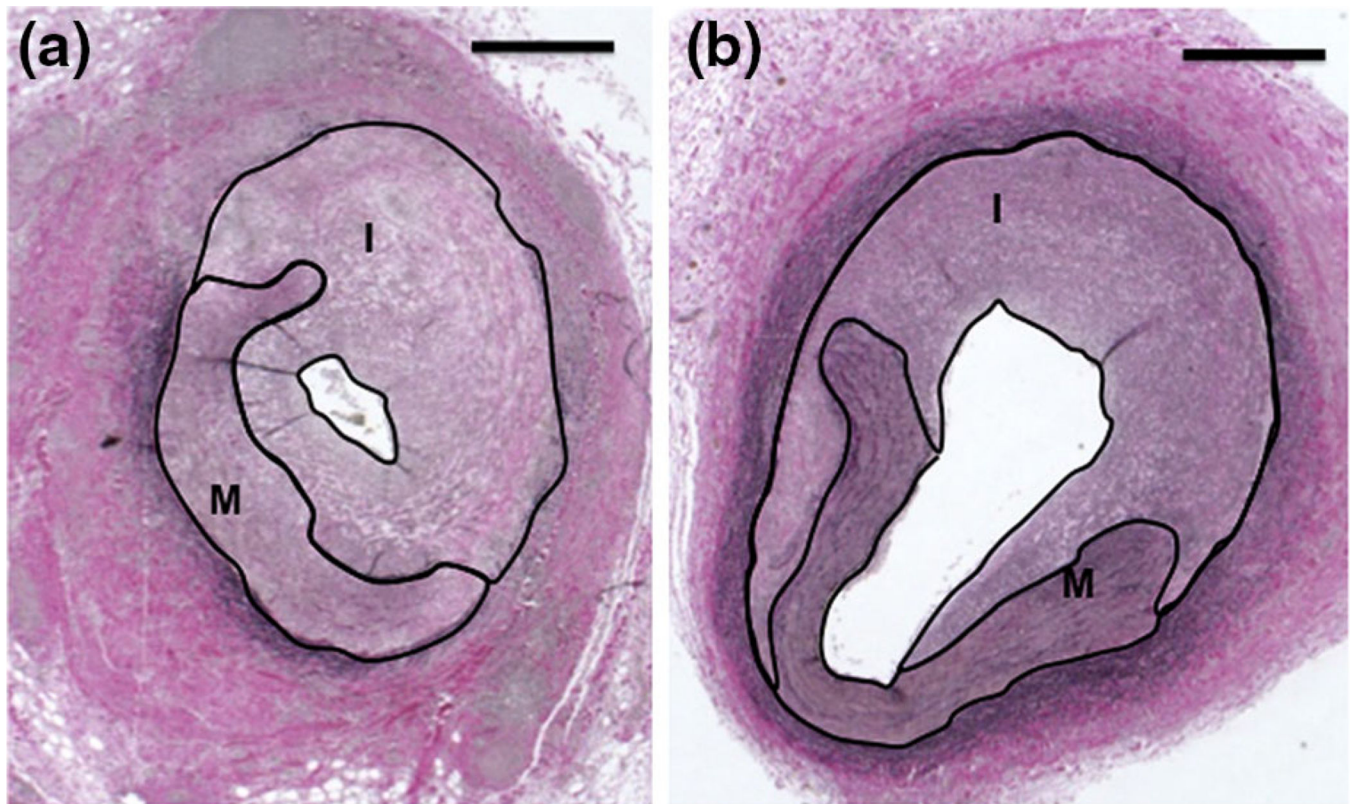


**FIGURE 5.** Representative images of histological sections following sirolimus-loaded microbubble infusion (a) without ultrasound and (b) with ultrasound. The area of the intima (I) and media (M) within each section is outlined. Scale bar = 500  $\mu\text{m}$ .

**TABLE 1**

Summary of the pulsing sequences applied in the *ex vivo* experiments.

	Time (s)									
	3	6	9	12	15	18	21	24	27	30
a. 2 MPa <sup>a</sup> only	2 MPa									
b. D <sup>a</sup> only	D									
c. D <sup>a</sup> + 1 MPa <sup>b</sup>	D      1 MPa      D      1 MPa									
d. D <sup>a</sup> + 2 MPa <sup>b</sup>	D      2 MPa      D      2 MPa									

Each treatment was repeated over a total of 60 s, with the same treatment in the first and second 30-s.

<sup>a</sup> Displacement pulses (D) were high duty cycle, low amplitude pulses.

<sup>b</sup> Burst pulses (1 & 2 MPa) were low duty cycle, high amplitude pulses.

Summary of the histology analysis comparing the treatment with microbubbles and ultrasound (MB + US) and microbubbles alone (MB – US).

**TABLE 2**

	MB + US samples	MB – US samples	IM ( <i>p</i> value) <sup>a,b</sup>	RI ( <i>p</i> value) <sup>a,b</sup>	IM/RI ( <i>p</i> value) <sup>a,b</sup>	IA ( <i>p</i> value) <sup>a,b</sup>	Ratio IM/RI <sup>b,c</sup>	Ratio IM <sup>b,d</sup>
Mean artery	7	5	0.106	0.202	0.0303	0.530	1.49	2.05
Max IM artery	7	5	0.0480	0.343	0.00505	0.202	2.03	2.87
Max RI artery	7	5	0.0480	0.343	0.0177	0.149	2.01	2.85

<sup>a</sup> Wilcoxon Rank Sum test *p* values comparing the MB + US and MB – US cases.

<sup>b</sup> IM intima to media ratio, RI rupture index, IM/RI = IM/RI, IA intima area.

<sup>c</sup> Ratio IM/RI = (IM/RI<sub>MB–US</sub>)/(IM/RI<sub>MB+US</sub>).

<sup>d</sup> Ratio IM = (IM<sub>MB–US</sub>)/(IM<sub>MB+US</sub>).